

The bow-shock and high-speed jet in the faint, 40 arcmin diameter, outer halo of the evolved Helix planetary nebula (NGC 7293)

J. Meaburn^{1*}, P. Boumis² & S. Akras²

¹*Jodrell Bank Centre for Astrophysics, University of Manchester, Oxford Rd., Manchester, UK. M13 9PL.*

²*Institute of Astronomy, Astrophysics, Space Applications and Remote Sensing, National Observatory of Athens, I. Metaxa & V. Pavlou, P. Penteli, GR-15236 Athens, Greece*

Accepted 2013 August 13. Received 2013 August 9; in original form 2013 June 29

ABSTRACT

In previous, very deep, optical images of NGC 7293 both a feature that has the morphology of a bow-shock and one with that of a jet were discovered in the faint 40' diameter halo of the nebula. Spatially resolved longslit profiles of the $H\alpha$ and $[N\text{ II}]$ 6548, 6584 Å nebular emission lines from both features have now been obtained.

The bow-shaped feature has been found to have $H\alpha$ radial velocities close to the systemic heliocentric radial velocity, -27 km s^{-1} , of NGC 7293 and is faint in the $[N\text{ II}]$ 6548, 6584 Å emission lines. Furthermore, the full width of these profiles matches the relative motion of NGC 7293 with its ambient interstellar medium consequently it is deduced that the feature is a real bow-shock caused by the motion of NGC 7293 as it ploughs through this medium. The proper motion of the central star also points towards this halo feature which substantiates this interpretation of its origin.

Similarly $[N\text{ II}]$ 6584 Å line profiles reveal that the jet-like filament is indeed a collimated outflow, as suggested by its morphology, at around 300 km s^{-1} with turbulent widths of around 50 km s^{-1} . Its low $H\alpha/[N\text{ II}]$ 6548, 6584 Å brightness ratio suggests collisional ionization as expected in a high-speed jet.

Key words: ISM: jets and outflows - planetary nebulae: individual (Helix NGC 7293)

1 INTRODUCTION

The evolved Helix (NGC 7293) planetary nebula (PN) is of particular importance because of its close proximity to the Sun and hence open to observation over an unprecedented range of spatial scales. Harris et al. (2007) measure a distance of only 219 pc to the white dwarf (WD 2226-210; Mendez et al. 1988) progenitor star which, with its surface temperature of 117,000 K radiatively ionizes the inner structure of the envelope ejected in its Asymptotic Giant Branch (AGB) phase to give the nebula a bright helical appearance at optical wavelengths. Originally a dMe late-type companion flare star in a central binary system (Gruendl et al. 2001) was thought to be present but later (Su et al. 2007) this was ruled out in favour of the presence of a 35-150 AU diameter debris disk around WD2226-210.

Observations of the morphology and kinematics of many of the structures up to a diameter of 25 arcmin of NGC 7293 have been made on a variety of spatial scales in many wavelength domains and these are summarised in Meaburn et al. (2005b), Meixner et al. (2005), Meaburn et al. (2008), Matsuura et al. (2009), Meaburn &

Boumis (2010), O'Dell, McCullough & Meixner (2004) & O'Dell, Henney & Ferland (2007) and references therein up to these dates. The consensus of opinion is that multiple eruptive events along different axes have occurred during the evolution of the central star as it passed from its AGB phase to its present WD state.

For instance Huggins & Healey (1986), Forveille et al. (1986) and Young et al. (1999) found two expanding molecular tori emitting the CO lines but with their axes orthogonal to each other: one axis is aligned with the inner bi-polar lobes that form the bright helical structure the other with the fainter lobes (L1 & L2 in Meaburn et al. 2008) that project into the halo. This complexity is not unexpected when other evolved PNe are considered e.g. see Guillén et al. (2013) for a recent example among many.

Jets of collimated ejected material are also not unexpected e.g. see those in the PN Fg 1 (López, Meaburn & Palmer 1993). Remarkably it was a very deep image in the light of the $H\alpha$ plus $[N\text{ II}]$ 6548, 6584 Å nebular emission lines obtained with the 30-cm aperture Crete optical telescope that revealed (see fig. 1c in Meaburn et al. 2005b) what appeared to be a bow-shock and a jet in the very outer 40 arcmin diameter faint halo of NGC 7293. Both of these morphological features were detected subsequently in the GALEX NUV (175- 280 nm) images and sketched in fig. 6 of Meaburn et

* E-mail: jmeaburn@jb.man.ac.uk

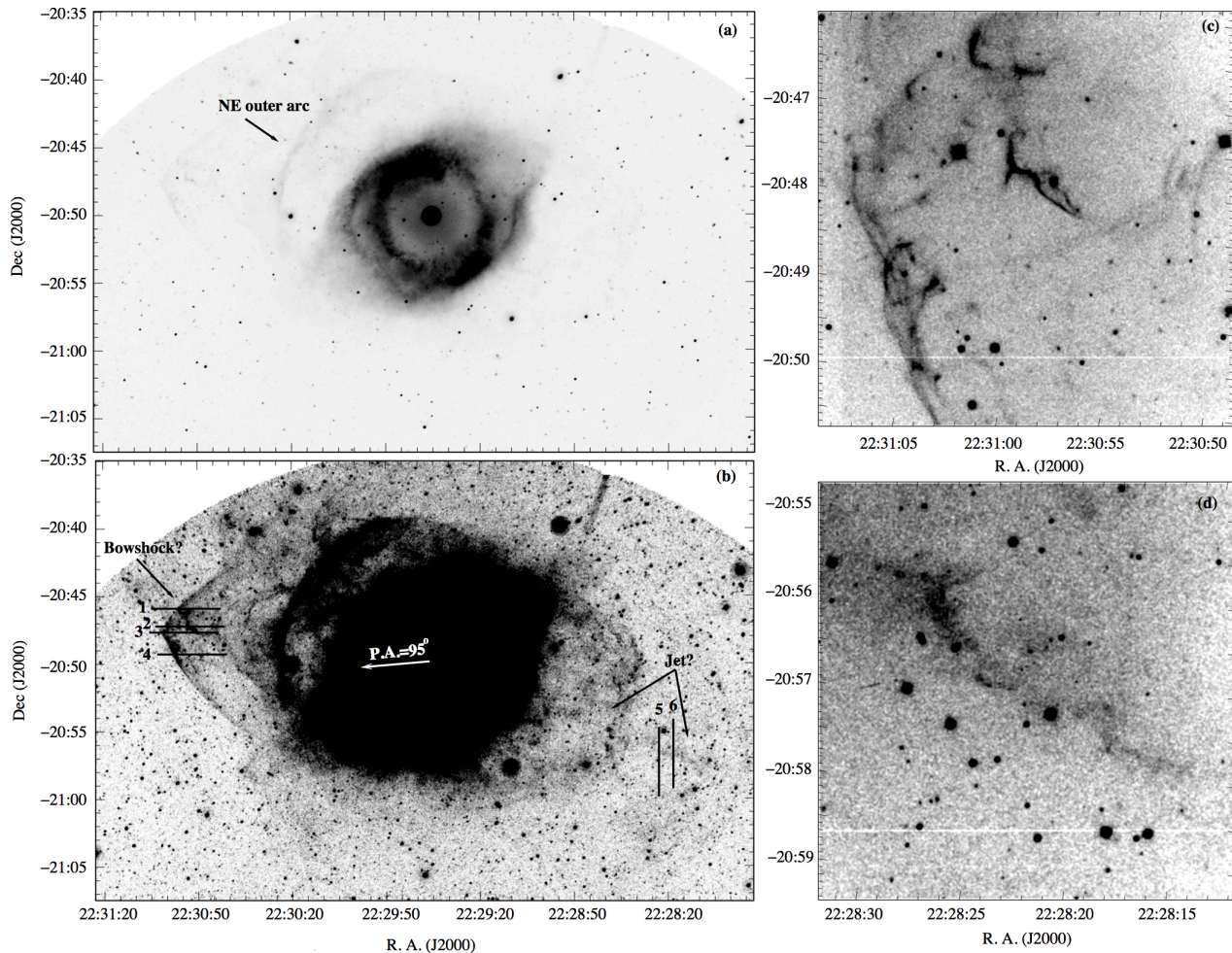


Figure 1. a) A light, negative, greyscale presentation of the GALEX NUV image. The NE outer arc is indicated. b) A deeper representation of the same image reveals both the NE bow-shaped feature with EW Slits 1 - 4 marked and the SW jet-like filament with the NS Slits 5 & 6 marked. The arrowed line over the central star indicates the direction of its proper motion. c) $H\alpha+[N II]$ image of the bow-shaped region and d) $H\alpha+[N II]$ image of the jet-like feature. The horizontal white line in c) and d) is a bad column on the ccd.

al. (2008) where the edge of this halo was called ‘outer envelope’. More recently the same outer features have been seen in the WISE all-sky-survey image of NGC 7293, at a wavelength of $12 \mu\text{m}$, by Zhang, Hsia & Kwok (2012).

Deep, spatially and spectrally resolved, longslit profiles of the $H\alpha$ and $[N II]$ 6548, 6584 Å emission lines have now been obtained over both this faint bow-shaped feature and that with a jet-like appearance in the outer halo of NGC 7293. Jets, in particular are expected to manifest themselves as high-speed, collimated outflows and should be easily verified unambiguously by their kinematical signature if tilted to the plane of the sky.

1.1 Observations

The longslit spectral observations were obtained with the second Manchester Echelle Spectrometer (MES–SPM; Meaburn et al. 2003) first used in La Palma but now installed at the $f/7.9$ focus of the 2.1-m San Pedro Martir UNAM telescope. This spectrometer has no cross-dispersion. For the present observations a filter of 90 Å bandwidth was used to isolate the 87th echelle order containing the nebular $H\alpha$ and $[N II]$ 6548, 6584 Å emission lines.

A Marconi e2v CCD with 2048×2048 square pixels, each

with $13.5 \mu\text{m}$ sides, was the detector. Two times binning was used in both the spatial and spectral dimensions consequently the 1024 increments along the slit length are each $0.352''$ long. A total projected slit length on the sky of $5.12'$ was therefore limited by the 30 mm length of the slit. ‘Seeing’ varied between $1-2''$ during these observations between 19-26 November 2012. The slit was $300 \mu\text{m}$ wide ($\equiv 20 \text{ km s}^{-1}$ and $3.8''$) and the integration time was 1800 s for each slit position. The spectra were calibrated to $\pm 1 \text{ km s}^{-1}$ accuracy against the Th/Ar arc lamp.

A light, negative, greyscale representation of the GALEX NUV image is shown in Fig. 1a to show the brighter central structures of NGC 7293. This can be compared in Fig. 1b with a deeper representation of the same image. The bow-shaped structure in the NE quadrant and the apparent jet-like feature to the SW can now be seen in Fig. 1b where the slit positions 1 – 6 for the present observations are marked. Details of the bow-shaped and jet like regions can be seen in the images in Fig. 1 c and d. These were obtained with the 2.3-m Aristarchos $f/8$ telescope at Helmos Observatory on August 6 and 9, 2013, through a 40 Å bandwidth filter centred on the $H\alpha+[N II]$ optical emission lines. Exposures of 1800 s duration were obtained with a 1024×1024 , $24 \mu\text{m}^2$ CCD detector ($\equiv 0.28$

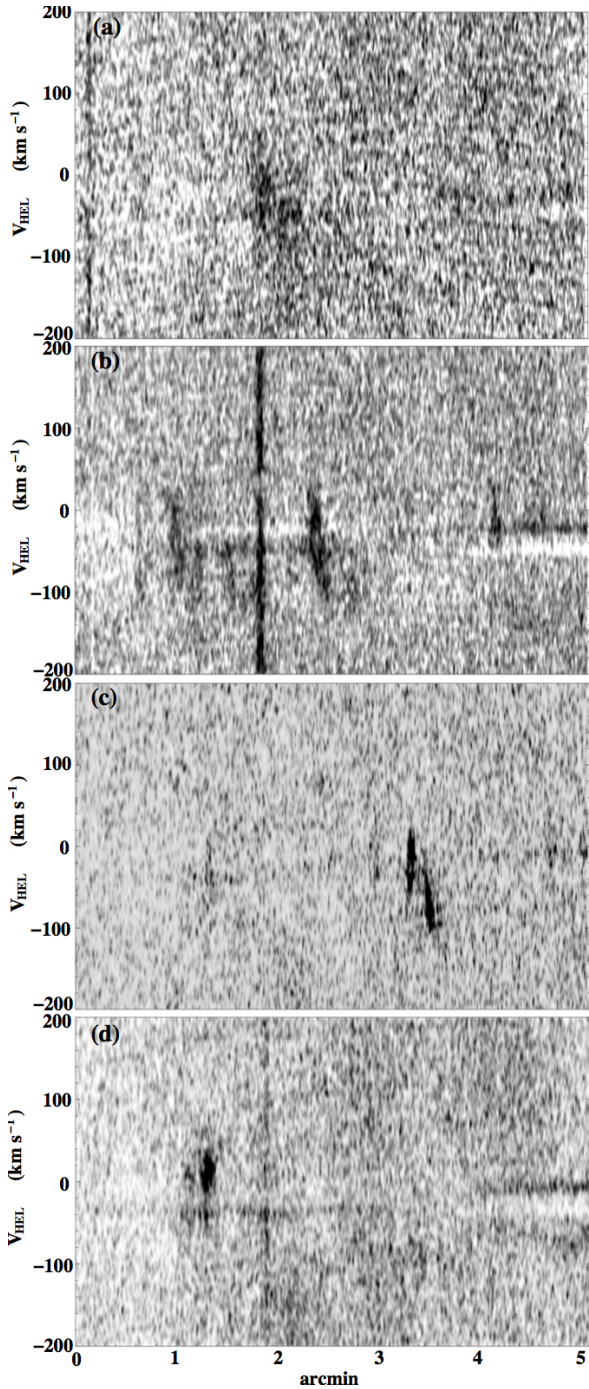


Figure 2. a)- d) show negative greyscale representations of the $H\alpha$ line profiles along the whole slit lengths 1-4 respectively which are marked in Fig. 1b. The dark vertical line in b) is the spectrum of a star. Faint horizontal features are the residuals of airglow lines after their partial subtraction from the data arrays.

arcsec²) resulting to a 5×5 arcmin² field of view. The image reduction was carried out using the IRAF and STARLINK packages.

2 RESULTS

2.1 NE bow-like feature

Negative grey-scale representations of the position-velocity (PV) arrays of $H\alpha$ profiles along the whole lengths of Slits 1-4, marked in Fig. 1b, are shown in Fig. 2 a-d respectively (and see the optical image in Fig. 1 c). The PV array of $H\alpha$ profiles along that part of EW Slit 3, which covers the brightest filament, is compared in Fig. 3 with an enlargement of the GALEX image in Fig. 1 for the region over NGC 7293 where it was obtained. The $H\alpha$ line profiles in Figs. 4 a & b are for the data in the incremental lengths A and B respectively marked in Fig. 3. Single Gaussian fits to these profiles have turbulent half-widths (fwhm) of 38 ± 3 km s⁻¹ and 49 ± 4 km s⁻¹ respectively when corrected for the 20 km s⁻¹ instrumental width, the 21.4 km s⁻¹ thermal width of the $H\alpha$ line at 10,000 K and the fine structural broadening of this line of 6.4 km s⁻¹. See Meaburn et al. (1991) for details of these corrections when applied to the observed $H\alpha$ and [N II] 6548, 6584 Å line profiles.

The A and B profiles are centred on $V_{\text{hel}} = -18 \pm 3$ and -73 ± 4 km s⁻¹ respectively. Their central values of V_{hel} should be compared to the systemic heliocentric radial velocity $V_{\text{sys}} = -27 \pm 2$ km s⁻¹ for the whole nebula (see fig. 8 in Meaburn et al. 2005b). The many other spectral features from the other slit positions over this eastern edge (the EW orientated Slits 1, 2 and 4 in Fig.1) can be seen in Fig. 2 a - d to have very similar widths and central values of V_{hel} as they cross the brighter filamentary edges of this eastern extreme of the outer halo of NGC 7293. Incidentally, the $H\alpha$ /[N II] 6548, 6584 Å brightness ratios are ≥ 4 for all of these filaments. Only one minor exception is found. That is for the small length of Slit 2 as it crosses the filament $\approx 1'$ west of the brightest filament in Fig. 3. Here the [N II] 6584 Å profile is centred on $V_{\text{hel}} = -67 \pm 3$ km s⁻¹ with a corrected width of 21 ± 2 km s⁻¹ and $H\alpha$ /[N II] 6548, 6584 Å brightness ratio ≤ 0.2 . This somewhat anomalous spectral feature is not detected in $H\alpha$ profiles in the same PV array but appears faintly in the [N II] 6548 Å nebular line profiles.

The $H\alpha$ line profile over the very apex of the bow-shaped feature is marginally detected in the most easterly parts of Slits 2 and 3 with about the same radial velocities and spectral half-widths of the profiles from incremental lengths A and B in Fig. 4a & b.

2.2 SW jet-like feature

The negative grey-scale representations of PV arrays of [N II] 6584 Å line profiles from the NS Slit 5 are compared in Fig. 5 with an enlargement of the GALEX NUV image that contains the jet-like feature. It can be seen that this feature emits the [N II] 6584 Å line over an 80'' length of the NS slit (and see the optical image in Fig. 1 d). Profiles from the incremental lengths A and B in Fig. 5 are shown in Figs. 6 a & b respectively. Single Gaussian fits to the profiles from A and B indicate turbulent widths (fwhm) of 53 ± 3 km s⁻¹ (fwhm) and 24 ± 2 km s⁻¹ respectively when both widths are corrected for the instrumental broadening of 20 km s⁻¹ and the [N II] 6584 Å (10000 K) thermal broadening of 5.7 km s⁻¹. Again see Meaburn et al. (1991) for details of these corrections but note that the [N II] 6584 Å line, unlike $H\alpha$, has no fine structural components and at a given temperature is thermally broadened by $14^{1/2}$ less than $H\alpha$.

The profiles from A and B are centred on $V_{\text{hel}} = 160 \pm 4$ km s⁻¹ and 170 ± 3 km s⁻¹ respectively. A similar, but fainter, spectral feature is seen along Slit 6 centred on $V_{\text{hel}} \approx 156$ km s⁻¹.

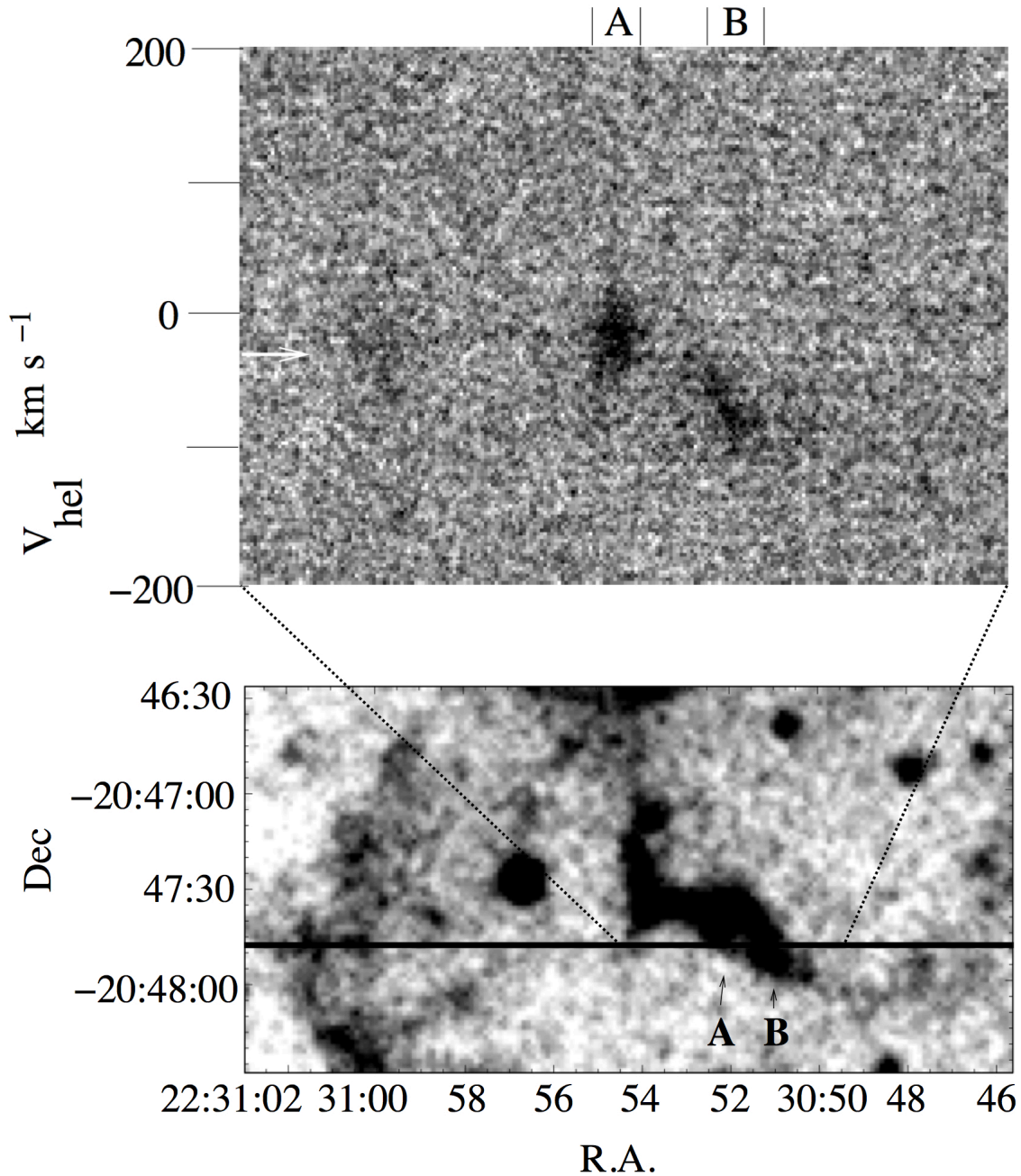


Figure 3. A negative greyscale representation of the position-velocity array of H α line profiles from the EW Slit 3 in Fig. 1b is compared with an enlargement of part of the GALEX NUV image which contains the NE bow-shaped region.

The corresponding spectral features in the [N II] 6584 Å line are only marginally detected in the H α line profiles in the same PV arrays which indicates a brightness ratio of H α /[N II] 6548, 6584 Å ≤ 0.2 . Again these central values of the profiles should be compared with $V_{\text{sys}} = -27 \text{ km s}^{-1}$ for the whole NGC 7293 nebula. Collimated jets with velocities of a few hundreds of km s^{-1} have also been found to other PNe (i.e. M 1-32; Akras & López 2012).

3 DISCUSSION

3.1 The jet

Undoubtedly the kinematics described in Sect. 2.2 of the linear emission line feature, tentatively identified in Meaburn et al. (2005b) from its morphology alone as a jet in the outer halo of NGC 7293, confirms this classification. Its measured radial velocity difference from V_{sys} of 192 km s^{-1} converts to an outflow velocity in a direction away from the central star of $V_j = 192/\sin(\theta) \text{ km s}^{-1}$ where θ is the angle of the jet to the plane of the sky. The low H α /[N II] 6548, 6584 Å brightness ratio of the jet's line emission

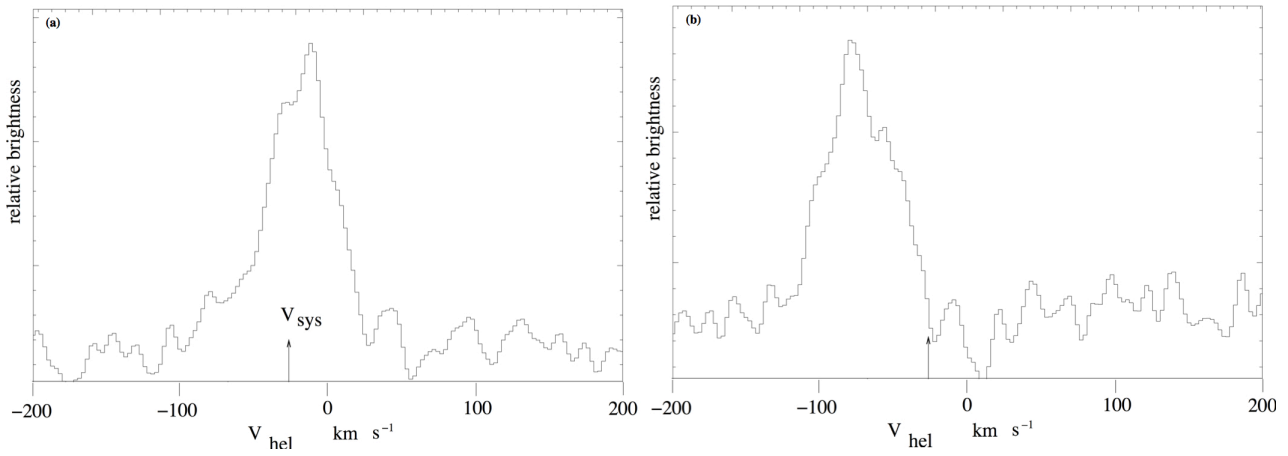


Figure 4. The $H\alpha$ line profiles from incremental lengths A & B marked in Fig. 3 are shown here in a) and b) respectively.

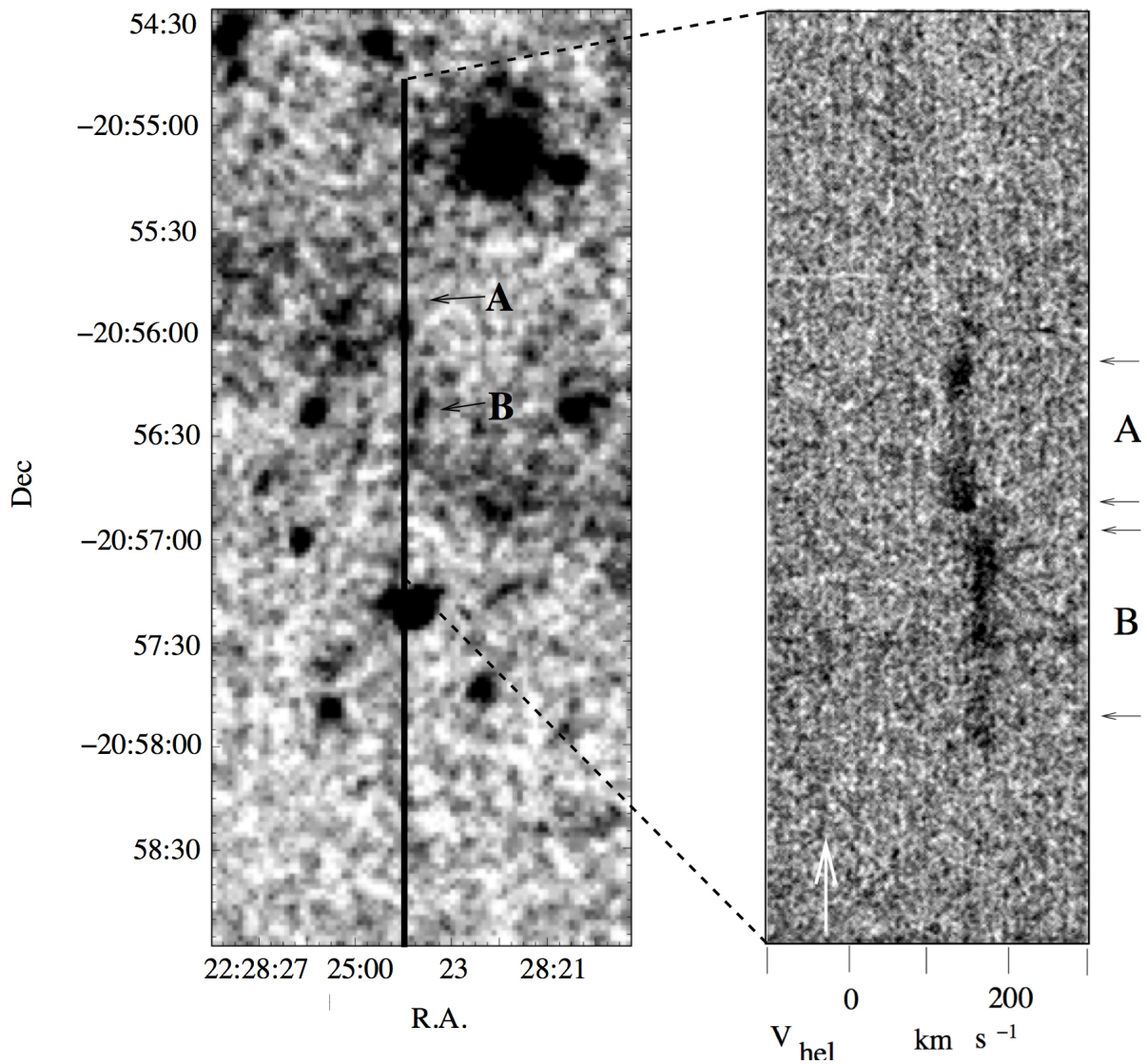


Figure 5. A negative presentation of the position-velocity array of $[N II] 6584 \text{ \AA}$ line profiles from the NS Slit 5 in Fig. 1b is compared with an enlargement of that part of the GALEX NUV image which contains the SW jet-like filament.

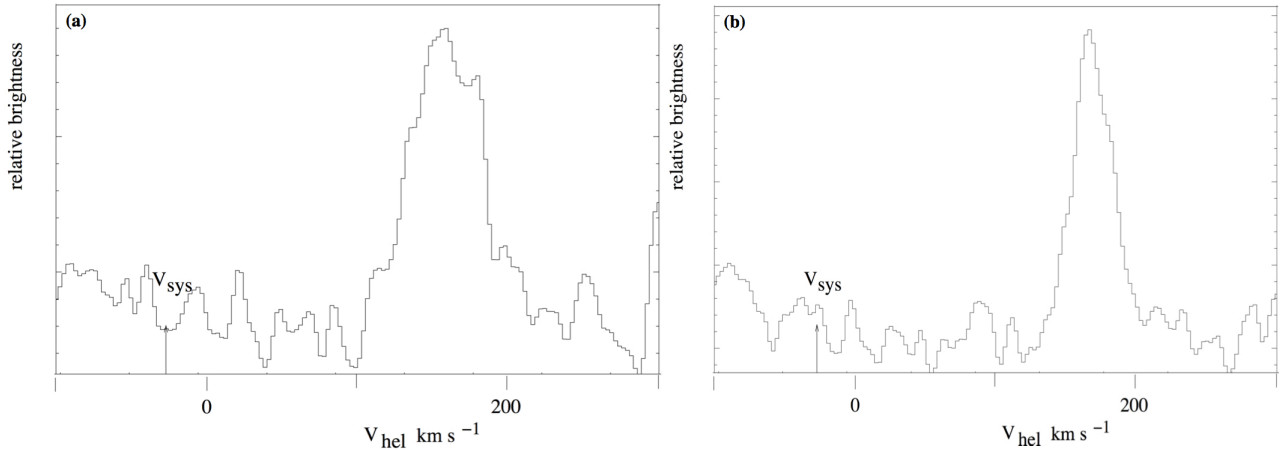


Figure 6. The [N II] 6584 Å line profiles for incremental lengths marked A & B in Fig. 5 are shown in a) and b) respectively.

also suggests that it is composed of collisionally ionized, nitrogen-enriched, collimated outflowing material originating in the star.

This jet extends to $23.8'$ from the central star and its tip is coincident with the furthest extent of the faint halo of NGC 7293 (called the ‘outer envelope’ in Meaburn et al. 2008). It may extend beyond this point but not encounter sufficiently dense material to produce its ionization, consequently a lower limit to its dynamical age is given by $T_d \geq 7400 \times \tan(\theta)$ yr for a distance to NGC 7293 of 219 pc. The value of θ can only be guessed at but a reasonable value of $\theta \approx 40^\circ$ gives $V_j \approx 300$ km s $^{-1}$ and $T_d \geq 6200$ yr. Within all of the uncertainties of applying this estimation to a jet this is comparable to $T_d = 10000$ yr estimated by Young et al. (1999) for the inner CO emitting torus.

The jet’s limited apparent length of $\approx 8'$ starting from the ‘SW outer arc’ (see Meaburn et al. 2008) of the halo of NGC 7293 suggests that it was a short-lived event in the evolution of the central star. It is interesting to speculate about the origin of this truncated jet within the evolutionary history of NGC 7293. Soker & Mcley (2013) show the presence of bi-polar jets in a pre-planetary nebula GRL 618 just before the ejection of the asymptotic giant branch (AGB) wind. Previously, Sahai & Trauger (1998), in their survey of young PNe revealed the presence of many jets in objects in the late AGB and/or early post-AGB evolutionary phases. It is therefore suggested that the, albeit mono-polar, jet detected in the present work had its origin in this early stage of the evolution of NGC 7293 and ceased as the AGB wind declined and the PN was born. This explanation would be consistent with the jet’s truncated nature. The tenuous evidence of a counter-jet in Sect. 2.2 and see Zhang, Hsia & Kwok (2012) needs to be investigated by further observations.

3.2 The bow-shock

As with the SW jet the kinematics of the bow-shaped feature in the NE quadrant of the outer halo of NGC 7293 can be the key to determine its origin. Its bow-shaped morphology makes it unlikely to be caused by ejected material from NGC 7293 (and see Sect. 3.3) therefore two further possibilities should be considered; it could either be a bow-shock ahead of an approaching counter jet to the receding one in the SW quadrant (Sect. 3.1) or a bow-shock caused as the whole of the NGC 7293 nebula ploughs through the ambient interstellar medium (ISM). If an as yet unseen approaching counter-jet exists, velocities in a bow-shock around its leading edge of a few hundreds of km s $^{-1}$ would be expected whereas, those for that

caused by the motion of NGC 7293 through the ambient medium would match the relative velocities. In fact, Hartigan, Raymond & Hartmann (1987) determined that the full-widths of emission lines from any bow-shocks caused by supersonic motions match their shock velocities.

The profiles from Slits 1–5 in Figure 1b whose examples are shown in Figs. 3 and 4a & b clearly (Sect. 2.1) have extents very much less than the ≈ 300 km s $^{-1}$ required if the bow-shaped feature is generated by a jet similar to that described in Sect. 3.1 consequently the magnitude of the relative motions of NGC 7293 with respect to its ambient medium must be explored.

Firstly, for the galactic longitude $l = 36.2060^\circ$ of NGC 7293 the effects of differential galactic rotation ($V_{\text{hel}} \leq 0.43$ km s $^{-1}$) are negligible. This then leaves the relative motion of NGC 7293 with respect to the ambient medium to be determined by a combination of the tangential velocity V_t of the central star WD2226-210 and the measured (Meaburn et al. 2005b) $V_{\text{sys}} = -27$ km s $^{-1}$ of the nebula. Using the proper motions of WD2226-210 determined by Cudworth (1974) and Kerber et al. (2008) along with the parallax distance of 219 pc of Harris et al. (2007) a value of $V_t = 40$ km s $^{-1}$ along position angle $\text{PA} = 95.7^\circ$ (marked on Fig. 1b) is given. The velocity of NGC 7293 with respect to its ambient medium is therefore $V_{\text{rel}} = 48$ km s $^{-1}$. Moreover, the PA of the PM of the central star points nearly directly to the apex of this bow-shaped feature (Fig. 1b) and the radial velocity of the apex is close to V_{sys} of NGC 7293.

Hartigan, Raymond & Hartmann (1987) predicted the shape and extent of line profiles from radiative bow shocks as Herbig-Haro objects ploughed into their ambient medium. This situation is similar, though of course not identical, to that proposed here. NGC 7293 is moving at ≈ 48 km s $^{-1}$ with respect to the ambient interstellar gas. In the production of a bow shock in the latter this should be combined with the ≈ 30 km s $^{-1}$ expansion velocity. A radiative bow-shock in the ambient gas would therefore be expected to be generated by these combined velocities in the direction of motion determined by the proper motion of the central star. Hartigan, Raymond & Hartmann (1987), though again for Herbig-Haro objects, showed that the full width of the combined line profile from the shocked region is equal to the relative motion of the ‘piston’ and the ambient gas. If this idea is reasonably applied to NGC 7293, then the full width of line profiles should be ≈ 80 km s $^{-1}$. It can be seen in the PV arrays of H α profiles in Figs 2 a–d & 3 and the individual profiles from these in Figs. 4a &

b that their full widths are from $V_{\text{hel}} = -100$ to 20 km s^{-1} around $V_{\text{sys}} = -27 \text{ km s}^{-1}$. This range is comparable with the relative velocities and it therefore can be stated conclusively, as a consequence of the present kinematic measurements that a bow-shocked region caused by the passage of NGC 7293 through its local ISM is present (as suggested by Zhang, Hsia & Kwok 2012 on morphological grounds alone). Similar features in the outer halos of PNe are common (Meaburn et al. 2005a for NGC 6583, Boumis et al. 2009 for HFG1 and Wareing, Zijlstra & O'Brien 2007a,b).

3.3 Hubble-type expansion

It is shown in Meaburn et al. (2008) that the expansions of the inner and outer molecular tori, the system of cometary globules, the inner bipolar lobes culminating in the north-eastern outer arc ($12.5'$ radius marked in Fig. 1a) all follow a Hubble-type law i.e. their expansion velocities increase linearly with their distances from the central star with a gradient of $\approx 7 \text{ km s}^{-1}(\text{arcmin radius})^{-1}$. This indicates that these are phenomena ejected from the central star over a short period of time with the fastest travelling furthest.

The jet (Sect. 3.1) with its measured radial velocity of 192 km s^{-1} relative to V_{sys} and extending out to an apparent radius of $23.8'$ fails by a factor ≈ 2 to fit into this pattern but this is not too surprising for it has a completely different dynamical origin to that of the ejected shells and tori. However, a similar comparison strengthens the suggestion that the NE bow-shaped filament is a bow-shock generated by NGC 7293 ploughing through the local ISM (Sect. 3.2). Its furthest extent from the central star is $21'$ and if following the Hubble-law for the inner ejected material an expansion velocity of $\approx 150 \text{ km s}^{-1}$ would be expected. The largest expansion velocity possible from the present measurements (Sect. 2.2) is ≥ 5 times smaller than this. Not only is a counter-jet origin for the creation of this outer bow-shaped filament ruled out (Sect. 3.2) but also an ejected origin.

4 CONCLUSIONS

The jet-like feature in the SW outer quadrant of the giant halo of NGC 7293 is confirmed kinematically to have a jet origin for it has a collimated outflow velocity of $\approx 300 \text{ km s}^{-1}$.

This jet has an $\text{H}\alpha/[\text{N II}]$ 6548, 6584 Å brightness ratio of ≤ 0.2 which confirms its origin as collisionally ionized, nitrogen enriched, material from the progenitor star.

The limited length of the jet's collimated outflow suggests it was emitted before the inner helical structure of NGC 7293 was ejected.

The bow-shaped outer filamentary structure in the NE quadrant of the outer halo of NGC 7293 is confirmed kinematically as a bow-shock created as NGC 7293 ploughs through its ambient medium. This interpretation is also consistent both with the magnitude and direction of the PM of the central star.

ACKNOWLEDGEMENTS

JM is grateful for the hospitality of the National Observatory of Athens in April 2013 when this paper was initiated. PB would like to thank the staff at SPM and Helmos Observatories for their excellent support during these observations. The Aristarchos telescope operated on Helmos Observatory by the Institute of Astronomy, Astrophysics, Space Applications and Remote Sensing of the National

Observatory of Athens. GALEX (Galaxy Evolution Explorer) is a NASA Small Explorer, launched in 2003 April. We gratefully acknowledge NASAs support for construction, operation, and science analysis for the GALEX mission, developed in cooperation with the Centre National d'Etudes Spatiales of France and the Korean Ministry of Science and Technology.

REFERENCES

- Akras S. & López J. A., 2012, MNRAS, 425, 2197.
 Boumis P, Meaburn J., Lloyd M., Akas S., 2009, MNRAS, 396, 1186.
 Cudworth K. M., 1974, AJ, 79, 1384.
 Forveille T., Huggins P.J., Bachiller R. & Cox P., 1998, ApJ, 495, L111.
 Gruendl, Chu, Y.H., O'Dwyer, Guerrero 2001, AJ, 122, 308.
 Guillén P. F., Vázquez R., Miranda L. F., Zavala S., Contreras M. E., Ayala S., Ortis-Ambriz A., 2013, MNRAS, tmp, 1368.
 Kerber F., Mignani R. P., Smart R. L., Wicenc A., 2008, A&A, 479, 155.
 Harris, H.C., Dahn, C. & Canzian, B. et al., 2007, AJ, 133, 631.
 Hartigan P., Raymond J. & Hartmann L., 1987, ApJ, 483, L57.
 Huggins, P. J. & Healey, A. J., 1986, ApJ, 305, 29.
 López J. A., Meaburn J., Palmer J.W., 1993, ApJ, 415, 135L.
 Matsuura, M., Speck, A. K., McHunu, B. M., Tanaka, I., Wright, N. J., Smith, M. D., Zijlstra, A. A., Viti, S. & Wesson, R., 2009, ApJ, 700, 1067.
 Meaburn, J., Nicholson, R., Bryce, M., Dyson, J. E., Walsh, J. R., 1991, MNRAS, 252, 53.
 Meaburn J., López J. A., Gutiérrez L., Quiróz F., Murillo J. M., Valdéz J., Pedrayez M., 2003, Rev. Mex. Astron. Astrofis., 39, 185.
 Meaburn, J., Boumis, P., Christopoulou P. E., Goudis C. D., Bryce M., López, J. A., 2005a, Rev. Mex. Astron. Astrofis., 41, 109.
 Meaburn, J., Boumis, P., López, J. A., Harman, D. J., Bryce, M., Redman, M. P. & Mavromatakis, F., 2005b, MNRAS, 360, 963
 Meaburn, J., López, J. A. & Richer, M. G., 2008, MNRAS, 384, 497.
 Meaburn, J & Boumis, P., 2010, MNRAS, 402, 381.
 Mendez R. H., Kudritzki R. P., Herrero A., Husfield D., Groth H. G., 1988, A&A, 190, 113.
 Meixner, M., McCullough, P. R., Hartman, J., Minh, S. & Speck, A., 2005, AJ, 130, 1784.
 O'Dell, C. R., McCullough P. R. & Meixner, M., 2004, AJ, 128, 2339.
 O'Dell, C. R., Henney, W. J. & Ferland, G. J., 2007, AJ, 133, 2343.
 Sahai R. & Trauger J. T., 1998, ApJ, 116, 1357.
 Soker N. & Mcley, L., 2013, ApJ (in press), (arXiv:1307.0182).
 Su K.Y.L., Chu Y-H., Rieke G. H., Huggins P. J., Gruendl R., Napiwotzki, R., Rauch T., Latter W. B., Volk K., 2007, ApJ, 657, L41.
 Wareing C.J., Zijlstra, A. A., O'Brien, T. J., 2007a, MNRAS, 382, 1233.
 Wareing C.J., Zijlstra, A. A., O'Brien, T. J., 2007b, ApJ, 660, L129.
 Young K., Cox P., Huggins, P.J., Forveille T. Bachiller R., 1999, ApJ, 522, 387.
 Zhang, Y., Hsia, C. H., Kwok, S., 2012, ApJ, 755, 53.